arXiv:cond-mat/0508329v1 [cond-mat.mtrl-sci] 13 Aug 2005

First-principles calculation of intrinsic defect formation volumes in silicon

Scott A. Centoni,[1,2,*] Babak Sadigh,[2] George H. Gilmer,[2] Thomas J. Lenosky,[3] Tomás Díaz de la Rubia,[2] and Charles B. Musgrave[4,5]

[1] *Department of Materials Engineering, San Jose State University, San Jose, California, 95192*
[2] *Lawrence Livermore National Laboratory, Livermore, California, 94550*
[3] *Ohio State University, Columbus, Ohio 43210*
[4] *Department of Materials Science and Engineering, Stanford University, Stanford, California, 94305*
[5] *Department of Chemical Engineering, Stanford University, Stanford, California, 94305*

(Dated: Revision1.52, October 24, 2002, 00:11:11 UTC)

We present an extensive first-principles study of the pressure dependence of the formation enthalpies of all the know vacancy and self-interstitial configurations in silicon, in each charge state from -2 through $+2$. The neutral vacancy is found to have a formation volume that varies markedly with pressure, leading to a remarkably large negative value (-0.68 atomic volumes) for the zero-pressure formation volume of a Frenkel pair ($V+I$). The interaction of volume and charge was examined, leading to pressure–Fermi level stability diagrams of the defects. Finally, we quantify the anisotropic nature of the lattice relaxation around the neutral defects.

PACS numbers: 61.72.Bb,61.72.Ji,66.30.Hs

INTRODUCTION

Nearly perfect crystals of silicon are of great technological importance, yet silicon self-diffusion is still not completely understood. Unlike the situation in metals, the equilibrium concentrations of vacancies and self-interstitials in Si are believed to comparable, and very low, making detection of them problematic. Experimental data is fragmentary, and simulations do not all agree. Controversy remains over the relative importance of vacancies and interstitials to self-diffusion at different temperatures and the relative magnitudes of the migration enthalpy to the formation enthalpy of these defects [1, 2]. We set aside the possibility of diffusion by a direct exchange mechanism [3] due to the low prefactor that has been calculated [4]. Then the self-diffusivity of silicon is the sum of the diffusion of Si due to vacancies and due to interstitials,

$$D_{\mathrm{Si}} = c_V D_V + c_I D_I \tag{1}$$

where the atomic fraction $c_X = C_X/C_{\mathrm{Si}}$ and $C_{\mathrm{Si}} = 5.00\times10^{22}\,\mathrm{cm}^{-3}$. The contribution of vacancies to Si diffusion is proportional to the concentration of vacancies C_V and the diffusivity of vacancies D_V, and likewise for interstitials. The equilibrium concentration of a defect X is $C_X^{\mathrm{eq}} = C_{\mathrm{Si}} \exp\left(-g_X^{\mathrm{f}}/k_BT\right)$, where g_X^{f} is the Gibbs free energy of formation of one defect. The diffusivity of a vacancy can be written as $D_V = (\zeta/6)\lambda^2 \nu_0 \exp\left(-g_V^{\mathrm{m}}/k_BT\right)$, where ζ is the coordination number, λ is the bond length, ν_0 is an attempt frequency, and g_V^{m} is the Gibbs free energy for the vacancy to exchange with one of its neighbors. The diffusivity of self-interstitials can be written similarly, but with a different geometric factor. Of course, $G = H - TS$, and if the entropy and enthalpy are assumed to be constant with respect to temperature, entropy may be combined with the pre-exponential factor, leaving only the enthalpy as a model parameter in the exponent.

Recent isotope tracer experiments [2] fit equilibrium silicon self-diffusivity to a single Arrhenius term

$$D_{\mathrm{Si}}^{\mathrm{eq}} = D_{\mathrm{Si}}^{\mathrm{eq0}} \exp\left(-\frac{h_{\mathrm{Si}}^{\mathrm{d}}}{k_BT}\right) \tag{2}$$

with $D_{\mathrm{Si}}^{\mathrm{eq0}} = 530^{+250}_{-170}\,\mathrm{cm}^2/\mathrm{s}$ and $h_{\mathrm{Si}}^{\mathrm{d}} = 4.75\pm0.04\,\mathrm{eV}$, suggesting that either vacancies or self-interstitials dominate self-diffusion over the entire temperature range studied—or instead that they switch over from one to the other but with similar values of $h_{\mathrm{Si}}^{\mathrm{d}}$. Of course, vacancies and self-interstitials diffuse by exchanging with lattice atoms, and thus cannot be isotopically tagged.

The concentrations C and diffusivities D of vacancies in silicon are difficult to measure separately with any accuracy, and likewise with self-interstitials. Estimated equilibrium transport capacities $c_X^{\mathrm{eq}} D_X = d_X^0 \exp\left(-\left(h_X^{\mathrm{f}} + h_X^{\mathrm{m}}\right)/k_BT\right)$ have been derived from experimental studies of metal diffusion in silicon, the most recent of which report values of $h_V^{\mathrm{f}} + h_V^{\mathrm{m}}$ ranging from 4.03 eV to 4.14 eV, and $h_I^{\mathrm{f}} + h_I^{\mathrm{m}}$ from 4.84 eV to 4.95 eV [2, 5]. On the other hand, the latest published work utilizing dopant diffusion arrives at an estimate of $h^{\mathrm{d}} = h_V^{\mathrm{f}} + h_V^{\mathrm{m}} = 4.86$ eV and $h^{\mathrm{d}} = h_I^{\mathrm{f}} + h_I^{\mathrm{m}} = 4.68$ eV [1], contrary to the long-held assumption that $h_I^{\mathrm{d}} > h_V^{\mathrm{d}}$. Ion implantation, thermal oxidation, and nitridation increase the concentration of intrinsic defects above their equilibrium concentrations ($C_X \gg C_X^{\mathrm{eq}}$), increasing the self- and dopant diffusivity; however, measuring activation enthalpies from such experiments requires assumptions about traps and other simplifications to differentiate between interstitial and vacancy mechanisms.

First-principles methods can be used to separately calculate formation and migration enthalpies, among other quantities. The enthalpies can be obtained from the energies calculated at different volumes as $H = E + PV + q\varepsilon_{\mathrm{F}}$, where ε_{F} is the Fermi level and q is the charge of the defect in electron units. Since $V = \partial H/\partial P$, the formation volume v_X^{f} tells us how the

formation enthalpy h_X^{f}, and thus the equilibrium concentration varies with pressure. Similarly, v_X^{m} tells us how much pressure enhances or retards the migration of a defect once it has entered the lattice. This is of technological interest because of the large stresses and strains that exist near the surfaces and interfaces of silicon-based integrated circuits (*e.g.* heteroepitaxial growth of Si upon $\mathrm{Si}_{1-x-y}\mathrm{Ge}_x\mathrm{C}_y$ or dielectric substrates), which may have a strong effect on concentrations and diffusion of intrinsic defects.

METHODS

Total energies were calculated using density functional theory (DFT), as implemented in the code VASP [6–9]. All calculations were performed with the PW91 exchange–correlation functional. Ion cores were represented with Vanderbilt ultrasoft pseudopotentials, allowing plane-wave energy cutoffs of 11 Ry = 150 eV. The Brillouin zone was sampled with **k** points equivalent to a 4×4×4 Monkhorst–Pack mesh in a conventional cubic (8-atom) cell. Periodic boundary conditions were used with primitive (2-atom) silicon cells for calculation of pure silicon and larger (mostly 128- or 256-site) supercells for calculations involving defects.

Our reference point was perfect silicon in the diamond cubic structure. The total energies at different volumes were fit to a Birch–Murnaghan equation of state [10]. In our calculations, silicon had a cohesive energy of 4.53 eV and equilibrium atomic volume $v_{\mathrm{Si}} = 20.34\,\text{Å}^3$. The bulk modulus at $P = 0$ was $B_0 = 0.88$ Mbar and its pressure derivative was $B_0' = 4.02$.

Similar calculations were performed with supercells containing defects. In each case, the supercells were set at a particular volume (scaled isotropically from the perfect lattice) and the ionic coordinates were fully relaxed to build up a list of at least seven energy–volume data points. Then the same equation of state was fit to the energy–volume data to find the enthalpy–pressure relationship. We define h_{Si} as the total enthalpy and v_{Si} as the volume of a silicon atom in the perfect crystal. A supercell containing 256 lattice sites and a vacancy includes 255 silicon atoms, so we define the formation enthalpy of a vacancy as $h_V^{\mathrm{f}} \equiv H_V[\mathrm{Si}_{255}] - 255h_{\mathrm{Si}}$, and likewise the formation volume is $v_V^{\mathrm{f}} \equiv V_V[\mathrm{Si}_{255}] - 255v_{\mathrm{Si}}$. Similarly, for self-interstitials $h_I^{\mathrm{f}} \equiv H_I[\mathrm{Si}_{257}] - 257h_{\mathrm{Si}}$ and $v_I^{\mathrm{f}} \equiv V_V[\mathrm{Si}_{257}] - 257v_{\mathrm{Si}}$. On the other hand, the quantities of interest in elasticity are the relaxation volumes $v_X^{\mathrm{rel}} \equiv V_X[\mathrm{Si}_{256\pm1}] - 256v_{\mathrm{Si}}$. The defects described in this work are shown in Figure 1 and will be commented on later.

VACANCIES

Intuitively, the simplest point defect is a neutral lattice vacancy, which we will label V_L^0: removing an atom from a perfect lattice. However, the neighboring atoms will tend to rebond in ways that make the defect less symmetric, particularly in a covalently bonded crystal like silicon. If the atoms are forced to maintain a T_d symmetry, the four neighbors draw in toward the center, pulling the rest of the lattice with them. However, the ground state involves a $T_d \to D_{2d}$ symmetry-breaking relaxation explained in the early days of quantum chemistry by Jahn and Teller [11]. The Jahn–Teller distortion of the neutral lattice vacancy in Si is now well-established by experiment [12] and theory [13]. We can see in Figure 2 the splitting of the triply degenerate T_2 level (occupied by two electrons) into a filled lower level and two degenerate empty upper levels, all still in the band gap.

Figure 3 shows that the Jahn–Teller distortion reduces the enthalpy of the defect by about 0.25 eV at $P = 0$, and results in a further contraction of $0.40v_{\mathrm{Si}}$. As a result, the formation

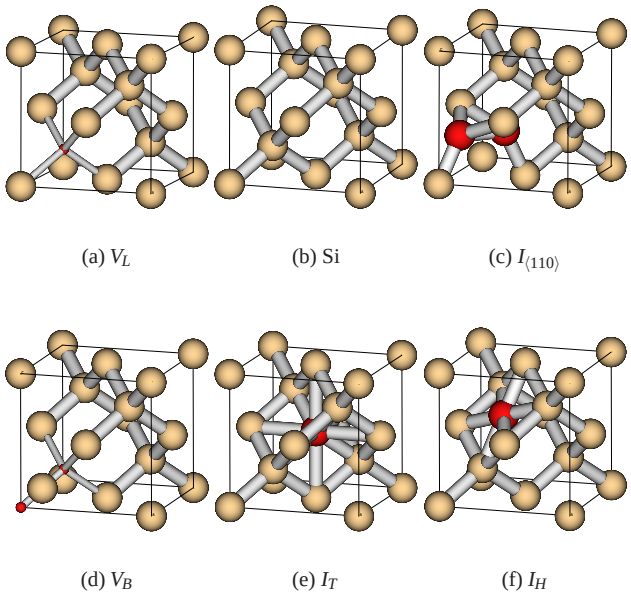

FIG. 1: **Geometries of defects** in relation to a conventional cubic unit cell of Si

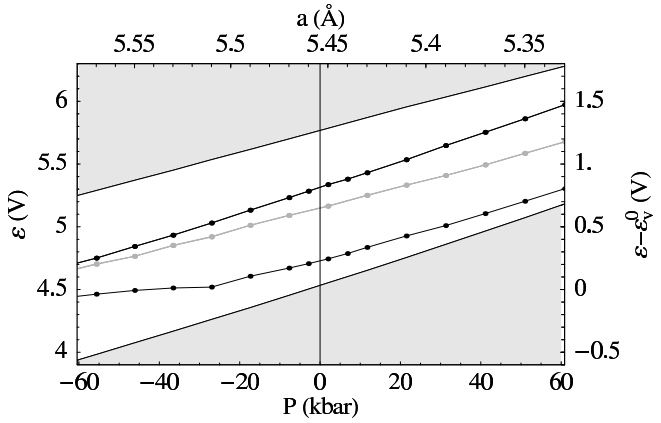

FIG. 2: **Jahn–Teller splitting of energy eigenvalues.** Shown are the band edges and the defect levels for V_L^0 with T_d (*gray*) and V_L^0 with D_{2d} (*black*) symmetry. Pressures are approximate.

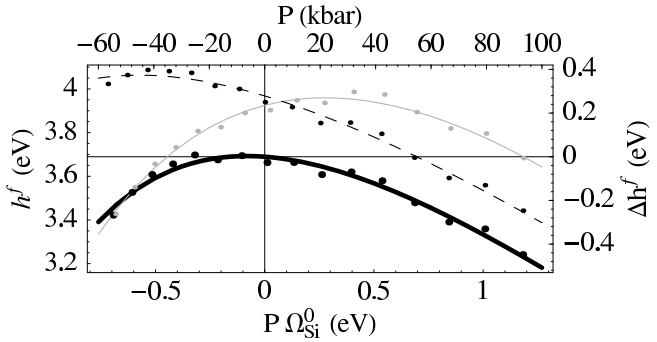

FIG. 3: **Effect of pressure on formation enthalpy of neutral vacancies.** Shown here are curves for V_L^0 with both T_d symmetry (*gray*) and D_{2d} (*heavy*), as well as V_B^0 (*dashed*). Fermi level ε_F fixed at intrinsic level ε_i.

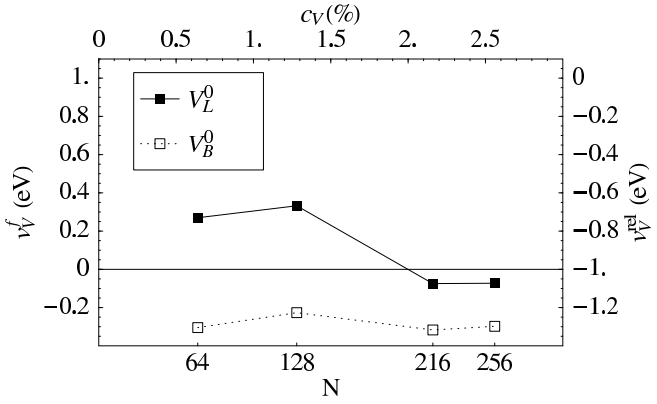

FIG. 4: **Effect of supercell size** on neutral vacancy (V^0) formation volume at $P = 0$ and $\varepsilon_F = \varepsilon_i$.

volume of a T_d vacancy is positive in our calculations, but that of a D_{2d} vacancy is a small negative value, $-0.07v_{Si}$ at $P = 0$, and vanishes at about -6 kbar. This surprising result implies that introducing vacancies into silicon (at $P = 0$) actually reduces the volume of the system and increases its density. A lattice with no relaxation would have $v_V^f = +v_{Si}$, while perfect relaxation (as with an incompressible liquid) would give $v_V^f = 0$.

The Jahn–Teller splitting vanishes under sufficiently large tensile strain, but is approximately constant under compressive strain. Other first-principles calculations of V_L^0 (though performed only for $P = 0$) have also reported small negative formation volumes [14]. In simulations reported in the literature, this distortion is stable only when using supercells with more than 128 atoms [15]. Our own calculations confirm this, with a transition from tetrahedral to tetragonal geometry occurring between 128 and 216 atoms (Figure 4).

Another high-symmetry configuration of $N-1$ atoms in a crystal with N sites is a so-called split vacancy, where one atom is at the bond center between two empty sites, a configuration we label V_B. This can easily be seen as a transition point for vacancy migration. Table I shows that V_B has a fairly constant large negative formation volume, about $-0.30v_{Si}$.

TABLE I: **Vacancy formation enthalpies and volumes** at $P = 0$ and $\varepsilon_F = \varepsilon_i$. ($v_V^f = v_{Si} + v_V^{rel}$)

	V_L^q		V_B^q	
q	h^f(eV)	$v^f(v_{Si})$	h^f(eV)	$v^f(v_{Si})$
-2	4.33	0.08	4.14	-0.27
-1	3.87	0.01	3.89	-0.30
0	**3.69**	**–0.07**	3.97	-0.30
$+1$	4.07	0.21	4.29	-0.37
$+2$	4.55	0.43	4.90	-0.42

However, in contrast to the lattice vacancy, this is not due to a Jahn–Teller symmetry breaking. As a result, the formation volume of the six-coordinated V_B^0 shows little change with supercell size (Figure 4) or pressure (Figure 3). From these arguments it also follows that the vacancy migration enthalpy is fairly constant for positive pressure, but increases for negative pressures.

We have also calculated the formation enthalpies and volumes of charged vacancies (Table I), since charged defects are expected to play an important role in doped silicon. Figure 5(a) shows that the neutral lattice-centered vacancy V_L^0 is the stable configuration over the broadest range of Fermi levels within the band gap (including the intrinsic level $\varepsilon_i = (\varepsilon_v + \varepsilon_c)/2$) and has a formation enthalpy of 3.69 eV at $P = 0$. The bond-centered split vacancy V_B^0 is 0.27 eV higher.

As mentioned above, V_B is the transition point for a vacancy to migrate from one V_L configuration to the next. However, our calculations reveal a surprising twist: The negative split vacancy V_B^- has almost the same energy as the negative lattice vacancy V_L^-, and at high Fermi levels, the ground state is in fact the split vacancy (the doubly negative split vacancy is even lower in energy than the lattice vacancy). This phenomenon was predicted decades ago by Bourgoin and Corbett [16], but is not well-known by all who work with silicon diffusion, since most industrially useful processes involve elevated temperatures. This reversal may be due to the greater number of bonds that can accept extra electrons in the case of the split vacancy. Since the displaced atom in the split vacancy has four valence electrons and six neighbors, giving the system two extra electrons allows this atom to form six equally strained bonds with all of its neighbors. In other words, the minimum-enthalpy geometry in one charge state (-2) is a saddle point in a different charge state (0), and vice versa. This crossover in potential energy surface is the requirement for the Bourgoin mechanism of athermal (electronically or optically activated) diffusion to take place [16, 17]. Experiments have demonstrated that vacancies in *n*-type silicon can diffuse at room temperature or even cryogenic temperature when subjected to optical or electronic excitation [12, 18].

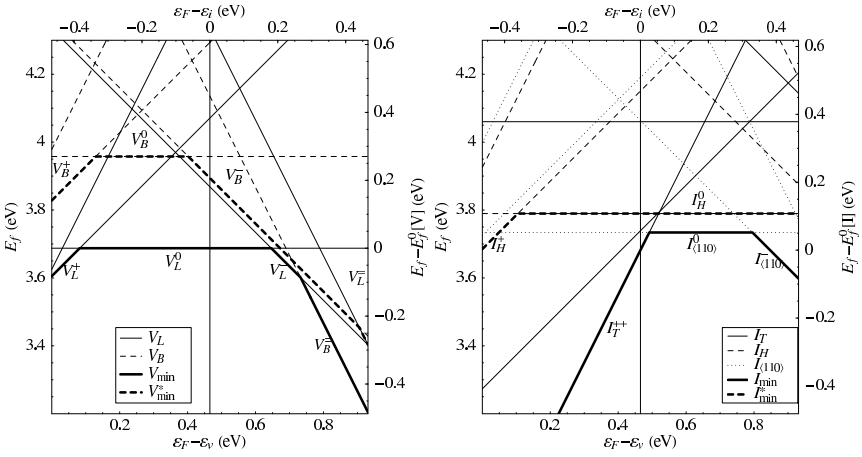

(a) Vacancies (b) Interstitials

FIG. 5: **Intrinsic defect formation enthalpies *vs.* Fermi level** at $P = 0$. The heavy solid line indicates the lowest formation enthalpy h^{f} for a defect at that Fermi level. The heavy dashed line indicates the second-lowest enthalpy, which is an estimate of h^{d}, the activation enthalpy of the transport capacity. The difference between the lines would then be the activation enthalpy of migration, h^{m}. Note that slope is proportional to the charge of the defect. A vertical line marks the calculated location of the intrinsic Fermi level ε_{i}.

SELF-INTERSTITIALS

We have calculated the enthalpies of the three interstitial geometries found to have the lowest enthalpies in previous work: tetrahedral (I_T), hexagonal (I_H), and split-$\langle 110\rangle$ ($I_{\langle 110\rangle}$). Our self-interstitial calculations are summarized in Table II. In contrast to the strong pressure and Fermi level sensitivity of vacancies, self-interstitials present a somewhat simpler picture. The lowest enthalpy interstitial at the intrinsic Fermi level and $P = 0$ is I_T^{++}, with a formation enthalpy of 3.68 eV and a formation volume of $-0.51 v_{\mathrm{Si}}$. (See the Methods section for an explanation of how formation enthalpies and volumes are defined in our calculations.)

We can explain the stability region of the various self-interstitial configurations, by plotting their formation enthalpies as a function of Fermi level (Figure 5(b)). We see that the I_T^{++} configuration is stable mainly in *p*-type Si, while at slightly elevated Fermi levels (*n* doping) the $I_{\langle 110\rangle}^0$ split interstitial is stabilized. A strong negative-*U* effect is seen, where the interstitial is nowhere stable in the $+1$ charge state.

Much like the situation with vacancies, high-symmetry interstitial geometries can be saddle points for interstitial migration. In particular, the hexagonal interstitial is usually assumed to be the migration point for interstitial diffusion. Figure 5(b) suggests that this is true for Si at almost any doping; hence interstitial migration in *n*-doped Si ($I_{\langle 110\rangle}^0 \rightarrow I_H^0 \rightarrow I_{\langle 110\rangle}^0$) has a migration barrier of only 0.06 eV, while in *p*-doped Si the migration mechanism $I_T^{++} \rightarrow I_H^+ \rightarrow I_T^{++}$ leads to a barrier that increases linearly with the doping level, thus causing a drastic slow-down of interstitial migration.

A particularly interesting regime is that of the Fermi level being close to the midgap, where the I_T^{++} is only slightly lower in energy than the neutral $I_{\langle 110\rangle}^0$. It is easy to see that under such conditions, addition of electrons *e.g.*through electron irradiation, can lead to a mechanism without any activation barrier. This so-called Bourgoin mechanism of electrically, rather than thermally, activated diffusion is observed experimentally at cryogenic temperatures during electron irradiation of intrinsic Si. One of the implications of this is that annealing after ion implantation should be significantly faster in *n*-type silicon than in *p*-type.

TABLE II: **Self-interstitial formation enthalpies and volumes** at $P = 0$ and $\varepsilon_{\mathrm{F}} = \varepsilon_{\mathrm{i}}$. ($v_I^{\mathrm{f}} = -v_{\mathrm{Si}} + v_I^{\mathrm{rel}}$)

	I_T^q		I_H^q		$I_{\langle 110\rangle}^q$	
q	h^{f} (eV)	$v^{\mathrm{f}}(v_{\mathrm{Si}})$	h^{f} (eV)	$v^{\mathrm{f}}(v_{\mathrm{Si}})$	h^{f} (eV)	$v^{\mathrm{f}}(v_{\mathrm{Si}})$
-2	5.37	-0.73	5.12	-0.49	4.70	-0.45
-1	4.61	-0.67	4.34	-0.43	4.06	-0.42
0	4.06	-0.63	3.79	-0.38	3.73	-0.41
$+1$	3.73	-0.60	4.15	-0.41	4.19	-0.45
$+2$	**3.68**	**–0.51**	4.85	-0.49	4.92	-0.51

FRENKEL PAIRS

Combining the formation volumes of the most stable vacancy and self-interstitial configurations indicates that a Frenkel pair ($V + I$) should have a formation enthalpy of 7.39 eV and a formation volume of $-0.68 v_{\mathrm{Si}}$. At elevated Fermi levels (*i.e.* high *n* doping), the stable self-interstitial species becomes $I_{\langle 110\rangle}^0$, which would lead to a Frenkel pair

formation enthalpy of 7.44 eV and formation volume of $-0.48v_{\rm Si}$.

On the other hand, Huang diffuse x-ray scattering experiments performed by Ehrhart *et al.* [19, 20] have been taken to conclude that the formation volumes of Frenkel pairs (produced by 2.5 MeV e^- or 4.5 keV He implantation) are quite small, $0.1v_{\rm Si}$ or less. This result is based on the assumption that at cryogenic temperatures, electron irradiation generates a substantial number of Frenkel pairs with a separation distance of only about 8 Å.

The disagreement of the Erhart experiments with our first-principles calculations suggests that Frenkel pairs with short separation distances behave differently from the isolated defects. This is not an unreasonable theory when considering our previous findings (see section Vacancies) of the sensitivity of the formation volume of the vacancy to its concentration (see Fig. 4). To see whether vacancies and interstitials at close proximity can behave anomalously, we constructed supercells containing a self-interstitial and a vacancy approximately 8 Å apart. Two different interstitial geometries were used, I_T and $I_{\langle 110\rangle}$. Only neutral supercells were considered, since the claim of Ehrhart *et al.* is that irradiation of silicon creates large concentrations of Frenkel pairs that are either entirely neutral or form donor–acceptor pairs. In this case, the Frenkel pair would not consist of $V_L^0+I_T^{++}$, but perhaps of $V_L^0+I_{\langle 110\rangle}^0$, $V_L^-+I_T^+$, or $V_L^{--}+I_T^{++}$. Formation volumes are calculated as before. The results are shown in Table III, together with summed values for the isolated defects.

TABLE III: **Frenkel pair enthalpies and volumes of formation.** Values for isolated defects are summed for convenience.

geometry	r(Å)	$h^{\rm f}$(eV)	$v^{\rm f}(v_{\rm Si})$
$(V_BI_T)^0$	5.88	6.88	−0.89
$(V_LI_T)^0$	8.83	7.18	−0.63
$(V_LI_{\langle 110\rangle})^0$	8.21	7.31	−0.48
$V_L^0+I_{\langle 110\rangle}^0$	∞	7.44	−0.48
$V_L^0+I_T^{++}$	∞	7.39	−0.68
$V_L^{--}+I_T^{++}$	∞	8.04	−0.62

The formation volume for $V_L^0+I_{\langle 110\rangle}^0$ is nearly the same whether both defects are in the same supercell or calculated separately. The formation enthalpy is a bit lower for the pair than for the isolated defects, which indicates the strength of the their attraction. Interestingly, in the case of $(V_LI_T)^0$, the relaxation of the atoms surrounding the vacancy took the form of a bent square, rather than two pairs seen in the isolated vacancy, even when the symmetry was broken in the direction of the expected geometry. In summary, for either the T or $\langle 110\rangle$ geometry, the Frenkel pair formation volume is a sizable negative number, contrary to the experimental results of Erhart et al.

In light of this, the assertion of Erhart et al. that irradiation of Si at cryogenic temperatures will create a large number of Frenkel pairs with short separation distances is inconsistent with first-principles calculations. Instead, our calculations suggest that far more defect clustering occurs than would be expected from purely classical migration mechanism of neutral defects. For samples irradiated by electrons or light, the Bourgoin mechanism described in previously can lead to athermal diffusion. On the other hand, radiation damage from ions can deposit enough energy in a small volume to directly create clusters of defects or even amorphous pockets and local melting despite cryogenic background temperatures.

Besides the possibility of clustering even at low temperatures, $V-V$ interactions may provide another possible explanation of the low observed Frenkel pair formation volume. The largest supercell in our calculations that stabilized the T_d symmetry was the 128-site supercell, having $h^{\rm f}[V_L^0]=3.51$ eV and $v^{\rm f}[V_L^0]=0.34v_{\rm Si}$, (Figure 4), with larger values of each expected with a larger supercell size. This would imply that $h^{\rm f}[V+I]=7.21$ eV and $v^{\rm f}[V+I]=-0.24v_{\rm Si}$. Interestingly, summing with $I_{\langle 110\rangle}^0$ instead of I_T^{++} would lead to $h^{\rm f}[V+I]=7.26$ eV and $v^{\rm f}[V+I]=-0.04v_{\rm Si}$. A single defect in a 100-site supercell corresponds to a defect concentration of 1%. At sufficiently high vacancy concentrations, $V-V$ elastic interactions may destabilize the Jahn–Teller distortion, leading to a positive vacancy formation volume and a small Frenkel pair formation volume, as well as a lower formation enthalpy. The critical concentration to destabilize the Jahn–Teller distortion for actual vacancies in silicon need not lie in the interval $\frac{1}{128}<c_V<\frac{1}{216}$.

Some earlier experiments claimed to find that $c_VD_V=c_ID_I$ at $T=800\,^\circ$C [5] or $T=1000\,^\circ$C [2]. Near that temperature, the effective activation enthalpy of Si self-diffusion should be close to $\frac{1}{2}(h^{\rm d}[V]+h^{\rm d}[I])$. Our calculations indicate $h^{\rm f}[V]=3.69$ eV and $h^{\rm f}[I]=3.68$ eV under conditions of no doping or applied pressure. Our estimate of $h^{\rm m}[V]=0.27$ eV appears reasonable, but we take $h^{\rm m}[I]=0.22$ eV based on a study of low-symmetry pathways not investigated here [21]. Thus we arrive at $h^{\rm d}[V]=3.96$ eV and $h^{\rm d}[I]=3.90$ eV. These estimates are rather lower than most experimental reports. DFT methods predict migration enthalpies more accurately than they do formation enthalpies. Probably the most accurate method applied to the calculation of intrinsic defects in Si is diffusion quantum Monte Carlo (DMC), which gives $h^{\rm f}[I_H^0]=4.82$ eV [22], 1.02 eV greater than the PW91 value, and leads to $h^{\rm d}[I]=5.04$ eV.

PRESSURE–FERMI LEVEL STABILITY DIAGRAMS

Examining the combined effects of changing pressure and Fermi level requires finding the enthalpies and volumes of formation of electrons and holes in Si as a function of pressure. The enthalpies are essentially the conduction band minimum

$$h_{\rm e}^{\rm f}(P)\equiv H[{\rm Si}_N^{-1}](P)-Nh_{\rm Si}(P) \qquad (3)$$

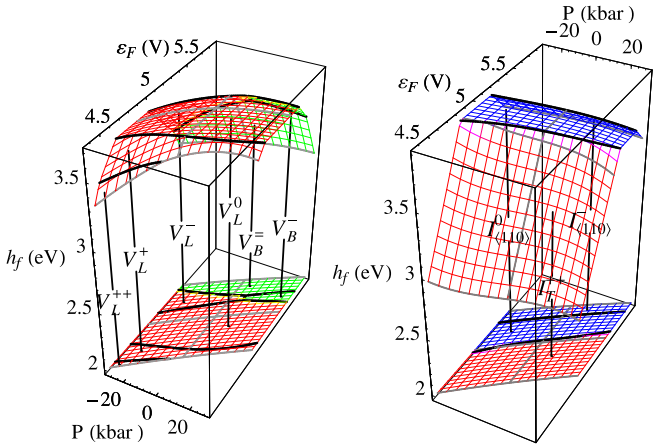

(a) Vacancy (b) Interstitial

FIG. 6: **Minimum formation enthalpy of defects as a function of P and ε_F).** The intrinsic Fermi level is indicated as a gray line.

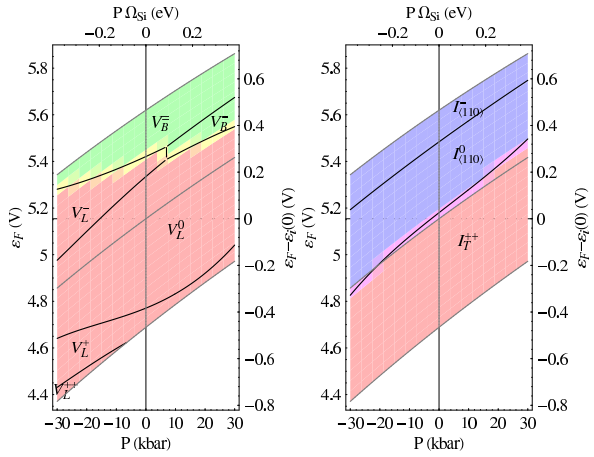

(a) Vacancy (b) Interstitial

FIG. 7: $P-\varepsilon_F$ **stability diagram of intrinsic defects in Si** formed by projecting the surface of minimum enthalpy in Figure 6 for V_L (red), V_B (green), I_T (red), I_H (green), and $I_{\langle 110\rangle}$ (blue). The intrinsic Fermi level is indicated as a gray line.

and the valence band maximum

$$h_{\rm h}^{\rm f}(P) \equiv N h_{\rm Si}(P) - H[{\rm Si}_N^{+1}](P). \tag{4}$$

and the volumes are

$$v_{\rm e}^{\rm f}(P) \equiv V[{\rm Si}_N^{-1}](P) - N v_{\rm Si}(P) = \frac{\partial \varepsilon_{\rm c}(P)}{\partial P} \tag{5}$$

and

$$-v_{\rm h}^{\rm f}(P) \equiv N v_{\rm Si}(P) - V[{\rm Si}_N^{+1}](P) = \frac{\partial \varepsilon_{\rm v}(P)}{\partial P}. \tag{6}$$

At $P=0$, we have $v_{\rm e}^{\rm f} = 0.679 v_{\rm Si}$ and $v_{\rm h}^{\rm f} = -0.788 v_{\rm Si}$, a sizable effect.

Since we have the pressure dependence of all these quantities, we can essentially sweep Figure 5 over a finite pressure range, where the domain of the plot is the band gap. Showing all the enthalpy surfaces obscures the most important information, the lowest enthalpy defects. More useful is a plot of just the minimum enthalpy required to form a defect at a particular pressure and Fermi level (Figure 6). The vacancy surface (Figure 6(a)) shows clear changes with pressure and marked curvature, indicating a variable formation volume, while the shape of the interstitial surface (Figure 6(b)) is close to being a prism. The location of the Fermi level is important for interstitials, but the pressure is not. Projecting these surfaces down onto the $(P,\varepsilon_{\rm F})$ plane reveals other differences. The vacancy stability diagram (Figure 7(a)) displays a wealth of features: the instability of V_L^{++} under pressure, the transition from V_L^- to V_B^-, and in general the large changes in vacancy levels caused by pressure. None of these features are evident for interstitials (Figure 7(b)).

RELAXATION VOLUME TENSORS

The stress state in integrated circuits is seldom hydrostatic. On the scale of the wafer it is typically biaxial due to surface oxidation or nitridation, but at a sub-micron scale becomes quite complicated, with enormous stress gradients. Aziz [23] has described the effect of the formation volume of defects in a film under biaxial stress, but points out that a full treatment requires more information about a defect than just its scalar volume. Many calculations of defects in silicon point out changes in the positions of the neighboring atoms, but this can provide only qualitative, not quantitative information about the complete elastic distortion caused by the defect. The present work fills this gap.

Among the features of the code used here is full relaxation of the vectors defining the supercell. This tells us how the shape as well as the size of the supercell change when a defect is formed. Were we dealing with a simple cubic cell changing isotropically from edge length L_0 to L, we could define the relaxation volume as

$$v^{\rm rel} = L_0^3 \ln\left(\frac{L}{L_0}\right)^3 \approx L_0^3 \left(\frac{L-L_0}{L_0}\right)^3. \tag{7}$$

Instead, we have three non-orthogonal vectors (forming a transformation matrix $\mathsf{L} = L_{ij}$) changing in arbitrary directions. We may generalize (7) as

$$\mathsf{v}^{\rm rel} = \det(\mathsf{L}_0) \ln\left(\mathsf{L}_0^{-1}\mathsf{L}\right) \approx \det(\mathsf{L}_0)\mathsf{L}_0^{-1}\left(\mathsf{L}-\mathsf{L}_0^{-1}\right) \tag{8}$$

The relaxation volume tensors defined in this way are equivalent to the strain dipole tensors

$$\lambda_{ij} = v_{ij}^{\rm rel}/v_{\rm Si} \tag{9}$$

TABLE IV: **Relaxation volume tensors v_{ij}^{rel} of neutral defects in Si** at $\sigma_{ij} = 0$ and $\varepsilon_{\mathrm{F}} = \varepsilon_{\mathrm{i}}$. The scalar part is indicated as well as the eigenvalues and corresponding principal directions. Scalar volumes in parentheses reflect the relaxation volumes calculated using the boundary conditions described previously (*i.e.* purely dilatational strain of the supercell).

vacancy	$v_i(v_{\mathrm{Si}})$	$\mathbf{n}_i$	interstitial	$v_i(v_{\mathrm{Si}})$	$\mathbf{n}_i$
V_L^0	-0.83	$[110]$	$I^0_{\langle 110\rangle}$	$+0.57$	$[110]$
-1.02	-0.82	$[1\bar{1}0]$	$+0.68$	$+0.09$	$[001]$
(-1.07)	$+0.63$	$[001]$	$(+0.59)$	$+0.02$	$[1\bar{1}0]$
V_B^0	-0.95	$[111]$	I_H^0	$+0.23$	$[2\bar{1}\bar{1}]$
-1.30	-0.18	$[2\bar{1}\bar{1}]$	$+0.64$	$+0.23$	$[01\bar{1}]$
(-1.30)	-0.18	$[01\bar{1}]$	$(+0.62)$	$+0.19$	$[111]$
			I_T^0	$+0.12$	$[111]$
			$+0.37$	$+0.12$	$[2\bar{1}\bar{1}]$
			$(+0.37)$	$+0.12$	$[01\bar{1}]$

discussed by Nowick and Berry [24] and closely related to the piezo-spectroscopic elastic dipole tensors

$$P_{ij} = C_{ijkl} v_{kl}^{\mathrm{rel}} \tag{10}$$

of Kröner [25] (where C_{ijkl} is the elastic modulus tensor of the material).

Using (8), we have calculated the full tensor volumes of relaxation of intrinsic defects in Si, which are mostly quite anisotropic. The results are more easily interpreted by diagonalizing the matrices to find the eigenvalues and principal directions, which we have compiled in Table IV. (Some of the defects have an axis of symmetry, leading to degeneracy of eigenvalues. As a result, the corresponding eigenvectors are not unique, and a different pair of directions in that plane could be chosen instead.) Useful methods of visualizing these tensors [26] include plotting the volume ellipsoids (Figure 8) defined by

$$\frac{x^2}{v_1^2} + \frac{y^2}{v_2^2} + \frac{z^2}{v_3^2} = 1 \tag{11}$$

and the volume director surfaces (Figure 9)

$$\frac{x^2}{v_1} + \frac{y^2}{v_2} + \frac{z^2}{v_3} = \pm 1 \tag{12}$$

where $+1$ is taken for expansion and -1 for contraction.

The sum of the eigenvalues—the scalar part of the tensor–is approximately equal to the scalar relaxation volume calculated previously. The principal directions and the signs of the eigenvalues are all in accord with intuition. We find that the neutral lattice vacancy has D_{2d} symmetry (at least at this pressure). The expansion in the $[001]$ direction makes its slightly negative scalar relaxation volume all the more noteworthy. The degree of anisotropy makes clear that scalar relaxation volumes are far from a complete picture of the defect displacement field: The split vacancy has a quite different C_{3v} symmetry, drawing all six of its neighbors in, mostly toward each other.

Among the self-interstitials, the I_T^0 is isotropic, and the I_H^0 is nearly so, pushing out a bit more in the (111) plane. The greatest component of the displacement around $I^0_{\langle 110\rangle}$ is, as expected, an expansion in the $[110]$ direction, but the other components are quite small. Two such interstitials, aligned in the same direction, will tend to repel if their axes are parallel to the line between them, and attract if the axes are perpendicular to the line between them. This suggests that clusters of these interstitials may agglomerate in a $\{110\}$ plane with their axes aligned to maximize their attraction. This long-range interaction may explain how interstitials are drawn together to form extended defects, including $\langle 110\rangle$ chains and eventually $\{311\}$ defects, as seems to be the case [27].

PREVIOUS WORK

First-principles calculation of the effect on intrinsic defect formation energies of changing lattice parameter was performed as early as 1984 by Car *et al.* [28] and LDA in 1989 by Antonelli and Bernholc [29], using supercells with 32 atoms. Those works did not include $I_{\langle 110\rangle}$. Sugino and Oshiyama [30] studied the effect of pressure on the diffusion of group V dopants (P, As, Sb) in silicon, but not silicon self-diffusion. Most published reports are limited to examining energy differences with a fixed volume.

Previous work by Zhu [31] and others [32] used the local density approximation (LDA), which does not include the gradient correction of GGA (generalized gradient approximation) methods such as PW91. GGA methods tend to predict energies of localized states (such as defects) with less error than LDA. Also, those calculations were limited to 64-site cells. However, it has been found necessary to use supercells containing over 200 atoms to stabilize the Jahn–Teller distortion of V_L^0 (cf. Puska *et al.* [15]).

CONCLUSIONS

We have performed first-principles calculations on a number of basic properties of intrinsic defects in silicon, some novel, some not presented together in a unified analysis before. The relaxation volumes of electrons and holes ($+0.68 v_{\mathrm{Si}}$ and $-0.79 v_{\mathrm{Si}}$, respectively) are an appreciable fraction of an atomic volume in magnitude. The formation enthalpy of a neutral vacancy is 3.69 eV and its migration enthalpy is 0.27 eV. The relaxation volume of the neutral vacancy, $-1.07 v_{\mathrm{Si}}$, is of the expected sign but the magnitude of the number is rather large, resulting in a formation volume of $-0.07 v_{\mathrm{Si}}$, with an activation volume of migration of $-0.24 v_{\mathrm{Si}}$. That is, hydrostatic pressure should lead to a slight *increase* in equilibrium vacancy concentration and an increase in vacancy diffusion. The most stable self-interstitial species,

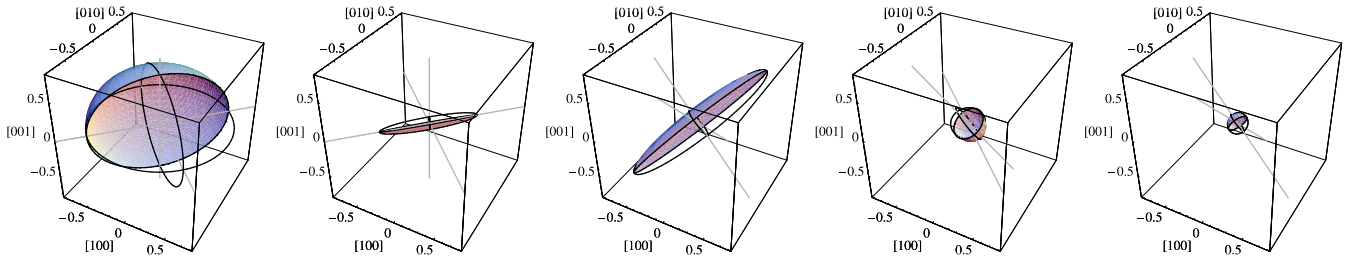

(a) V_L^0 (b) $I_{\langle 110\rangle}^0$ (c) V_B^0 (d) I_H^0 (e) I_T^0

FIG. 8: **Volume ellipsoids of neutral defects in Si** at $\sigma_{ij} = 0$ and $\varepsilon_F = \varepsilon_i$, as defined in Eq (11). Principal axes are indicated in gray.

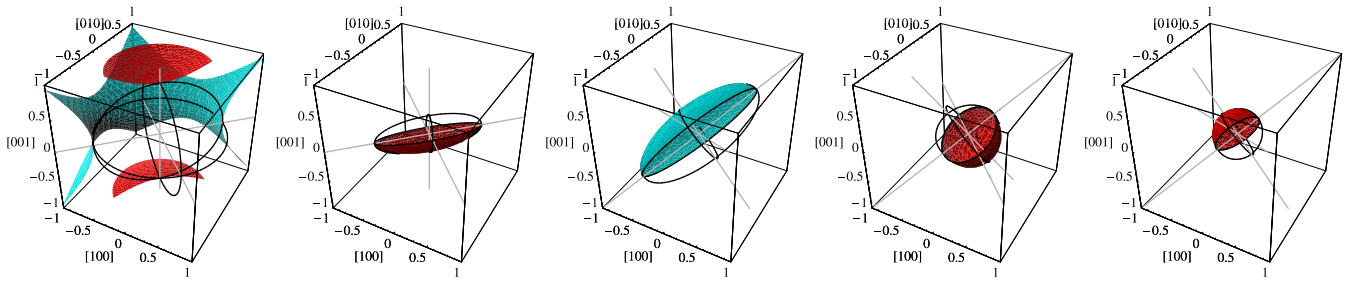

(a) V_L^0 (b) $I_{\langle 110\rangle}^0$ (c) V_B^0 (d) I_H^0 (e) I_T^0

FIG. 9: **Volume director surfaces of neutral defects in Si** at $\sigma_{ij} = 0$ and $\varepsilon_F = \varepsilon_i$, as defined in Eq (12). Surfaces of both expansion (*light blue*) and contraction (*red*) are shown. Principal axes are indicated in gray.

I_T^{++}, has a formation enthalpy 3.68 eV, equal to the formation enthalpy of V_L^0 within the accuracy of our method, and a formation volume of $-0.57v_{\mathrm{Si}}$ ($v^{\mathrm{rel}} = +0.43v_{\mathrm{Si}}$).

To estimate the concentration of a defect requires calculation of its vibrational and configurational entropy. The calculations we have performed do not provide this information, but the near equality of the formation enthalpies of the most stable vacancy and self-interstitial demand that the ratio C_I/C_V of their equilibrium concentrations should not vary much with temperature. The ratio will depend upon pressure, however. The formation volume of a Frenkel pair with no clustering or amorphization should be a sizable negative number, $-0.48v_{\mathrm{Si}}$ to $-0.68v_{\mathrm{Si}}$, unless interactions at high vacancy concentrations destabilize the Jahn–Teller distortion. These parameters should be of interest in studies of silicon under large elastic stresses. They imply that increasing hydrostatic pressure increases the equilibrium concentration of both vacancies and self-interstitials, though the effect on vacancy concentration should be weak. Increasing pressure should also increase the mobility of vacancies.

We have presented stability diagrams (akin to phase diagrams) of the intrinsic defects in silicon, showing the complexity of vacancies under pressure, in stark contrast to the behavior of self-interstitials. We have verified Bourgoin's prediction of a crossing in the vacancy potential energy surfaces.

Finally, we have calculated the full tensor relaxation volumes of these intrinsic defects, enabling researchers to model the biased diffusion of both vacancies and self-interstitials under the non-hydrostatic stress states found in actual devices.

This work was performed under the auspices of the U. S. Department of Energy by the University of California, Lawrence Livermore National Laboratory under Contract No. W-7405-Eng-48. Funding was provided by the Department of Energy Office of Basic Energy Sciences.

* Electronic address: scentoni@email.sjsu.edu

[1] A. Ural, P. B. Griffin, and J. D. Plummer, Phys. Rev. Lett. **83**, 3454 (1999).
[2] H. Bracht, E. E. Haller, and R. Clark-Phelps, Phys. Rev. Lett. **81**, 393 (1998).
[3] K. C. Pandey, Phys. Rev. Lett. **57**, 2287 (1986).
[4] K. C. Pandey and E. Kaxiras, Phys. Rev. Lett. **66**, 915 (1990).
[5] T. Y. Tan and U. Gösele, App. Phys. **A 37**, 1 (1985).
[6] G. Kresse and J. Hafner, Phys. Rev. **B 47**, 558 (1993).
[7] G. Kresse and J. Hafner, J. Phys.: Condens. Matter **6**, 8245 (1994).
[8] G. Kresse and J. Furthmüller, Comput. Mat. Sci. **6**, 15 (1996).
[9] G. Kresse and J. Furthmüller, Phys. Rev. **B 54**, 11169 (1996).
[10] F. D. Murnaghan, Proc. Natl. Acad. Sci. **30**, 244 (1944).

[11] H. A. Jahn and E. Teller, Proc. R. Soc. London A **161**, 220 (1937).
[12] G. D. Watkins, in [33], pp. 139–150.
[13] E. Tarnow, J. Phys.: Condens. Matter **5**, 1863 (1993).
[14] A. Antonelli, E. Kaxiras, and D. J. Chadi, Phys. Rev. **B 81**, 2088 (1998).
[15] M. J. Puska, S. Pöykkö, M. Pesola, and R. M. Nieminen, Phys. Rev. **B 58**, 1318 (1998).
[16] J. C. Bourgoin and J. W. Corbett, in *Lattice Defects in Semiconductors—1974*, edited by F. A. Funtley, Institute of Physics (Institute of Physics, Bristol, 1975), no. 23 in IOP Conference Proceedings, p. 149.
[17] J. C. Bourgoin and J. W. Corbett, Phys. Lett. **A 38**, 135 (1972).
[18] A. N. Larsen, C. Cristensen, and J. W. Petersen, J. App. Phys. **86**, 4861 (1999).
[19] P. Ehrhart and H. Zillgen, in [33], pp. 175–186.
[20] P. Partyka, Y. Zhong, K. Nordlund, R. S. Averback, I. M. Robinson, and P. Ehrhart, Phys. Rev. **B 64** (2001).
[21] R. J. Needs, J. Phys.: Condens. Matter **11**, 10437 (1999).
[22] W.-K. Leung, R. J. Needs, and G. Rajagopal, Phys. Rev. Lett. **83**, 2351 (1999).
[23] M. J. Aziz, Materials Science in Semiconductor Processing **4**, 397 (2001).
[24] A. S. Nowick and B. S. Berry, *Anelastic Relaxation in Crystalline Solids* (Academic Press, 1972).
[25] E. Kröner, *Kontinuumstheorie der Versetzungen und Eigenspannungen* (Springer, Berlin, 1958).
[26] S. Timoshenko and J. N. Goodier, *Theory of Elasticity* (McGraw–Hill, 1951), 2nd ed.
[27] J. Kim, J. W. Wilkins, F. S. Khan, and A. Canning, Phys. Rev. **B 55**, 16186 (1997).
[28] R. Car, P. J. Kelly, A. Oshiyama, and S. T. Pantelides, Phys. Rev. Lett. **52**, 1814 (1984).
[29] A. Antonelli and J. Bernholc, Phys. Rev. **B 40**, 10643 (1989).
[30] O. Sugino and A. Oshiyama, Phys. Rev. **B 46**, 12335 (1992).
[31] J. Zhu, in [33], pp. 151–162.
[32] W.-C. Lee, S.-G. Lee, and K. J. Chang, J. Phys.: Condens. Matter **10**, 995 (1998).
[33] T. Díaz de la Rubia, S. Coffa, P. A. Stolk, and C. S. Rafferty, eds., vol. 469 of *Materials Research Society Symposium Proceedings* (Materials Research Society, Warrendale, PA, 1997).